Plant Cell Rep (2012) 31:2247–2259
DOI 10.1007/s00299-012-1334-9

ORIGINAL PAPER

Overexpression of allene oxide cyclase promoted tanshinone/phenolic acid production in *Salvia miltiorrhiza*

Xiao-Ce Gu · Jun-Feng Chen · Ying Xiao · Peng Di · Hong-Jiao Xuan · Xun Zhou · Lei Zhang · Wan-Sheng Chen

Received: 12 April 2012 / Revised: 1 August 2012 / Accepted: 8 August 2012 / Published online: 29 August 2012

Abstract
Key message **This study provides a desirable candidate gene resource (*SmAOC*) to increase the content of valuable natural products via appropriate JA pathway genetic engineering.**
Abstract Jasmonates (JAs) are important signal molecules in plants. They regulate transcripts of defense and secondary biosynthetic metabolite genes in response to environmental stresses. Currently, JAs are widely used as elicitors to improve the content of useful secondary metabolism in plants. Synthesis of the naturally occurring enantiomer of various jasmonates is catalyzed by allene oxide cyclase (AOC, EC 5.3.99.6). Here, we cloned and characterized the AOC gene (*SmAOC*) from *Salvia miltiorrhiza*. As expected, *SmAOC* expression was induced by abiotic stimuli such as methyl jasmonate (MeJA), ultraviolet radiation (UV) and low temperature (4 °C) in *S. miltiorrhiza plantlets*. To demonstrate whether the engineered internal JAs pool by overexpressing *AOC* gene could promote secondary metabolism production, the *SmAOC* was incorporated into *S. miltiorrhiza* hairy roots. The results revealed that *SmAOC* overexpression significant enhanced the yields of tanshinone IIA, rosmarinic acid (RA) and lithospermic acid B (LAB) in *S. miltiorrhiza* hairy roots. In addition, expression levels for key genes involved in the biosynthetic pathway of diterpenes and phenolic acids were also altered. These suggest that genetic manipulation of AOC would be helpful for improving the production of valuable secondary metabolites by regulating the biosynthesis of JAs.

Keywords Allene oxide cyclase · Jasmonates · Secondary metabolism · Signal molecule · *Salvia miltiorrhiza*

Abbreviations

4CL	4-Coumarate coenzyme A ligase
AOC	Allene oxide cyclase
AOS	Allene oxide synthase
BV	Blank vector
CMK	Cytidine monophosphate kinase
CTAB	Cetyl trimethyl ammonium bromide
DXR	1-Deoxy-D-xylulose-5-phosphate reductoisomerase
HMGR	3-Hydroxy-3-methylglutaryl-CoA reductase
HPPR	4-Hydroxyphenylpyruvate reductase
hpt	Hygromycin phosphotransferase gene
IPTG	Isopropyl thiob-D-galactoside
JAs	Jasmonates
JMT	Jasmonic acid caboxyl methyltransferase
LAB	Lithospermic acid B
LOX	Lipoxygenase
MeJA	Methyl jasmonate
MRM	Multiple reactions monitoring

Communicated by E. Benvenuto.

X.-C. Gu · J.-F. Chen · Y. Xiao · P. Di · H.-J. Xuan · X. Zhou · W.-S. Chen (✉)
Department of Pharmacy, Changzheng Hospital, Second Military Medical University, Shanghai 200003, People's Republic of China
e-mail: chenw@vnet.citiz.net

L. Zhang
Department of Pharmacognosy, School of Pharmacy, Second Military Medical University, Shanghai 200433, People's Republic of China

L. Zhang (✉)
Department of Plant Sciences, University of California, Davis, CA 95616, USA
e-mail: zhanglei@smmu.edu.cn

ORF	Open reading frame
PAL	Phenylalanine ammonialyase
RA	Rosmarinic acid
RT-qPCR	Real-time quantitative PCR
TFs	Transcription factors
WT	Wild type

Introduction

The use of phytohormone jasmonates (JAs) to globally promote production of multiple primary and secondary metabolites may be an efficient alternative for enhancing accumulation of natural products (Jiang et al. 2009). Methyl jasmonate (MeJA) and its free acid, jasmonic acid (JA), are collectively referred to as JAs. JAs are lipid-derived hormones involved in the regulation of development, senescence, secondary metabolism, response to wounding and pathogens in plants (Chehab and Braam 2012). In response to abiotic and biotic stresses, JAs modulate a subset of defense genes with synergistic and antagonistic effects in relation to other plant hormones such as salicylate, ethylene and abscisic acid, through a signaling pathway (Robert-Seilaniantz et al. 2011). JAs can activate pathways leading to several classes of secondary metabolites, which are linked to plant defense against pathogens and herbivores (Wasternack 2007; Pauwels et al. 2009). Many transcription factors (TFs) often JA-activated themselves, with a role in the JA-modulated regulation of metabolism were discovered. At the same time, it became clear that metabolic reprogramming is subject to complex control mechanisms integrated in robust cellular networks (De Geyter et al. 2012). JAs could induce pathways synthesizing components of a wide structural variety, encompassing multiple branches of the most important secondary metabolite classes (Zhao et al. 2005). Therefore, MeJA has been widely employed to induce the biosynthesis of diverse secondary metabolism in plant tissue culture, for e.g. the accumulation of taxoid in *Taxus* (Ketchum et al. 1999) and the up-regulation of soyasaponin biosynthesis in *Glycyrrhiza glabra* (Hayashi et al. 2003).

Salvia miltiorrhiza, named Danshen in China, is one of the most important Chinese herbal drugs, which has been formulated and used clinically for promoting circulation and improving blood flow, e.g. angina pectoris, myocardial infarction and other cardiac symptoms (Zhou et al. 2005). Exogenous MeJA has been widely applied to accelerate the culture of many effective substances in *S. miltiorrhiza*. According to pharmacological investigations, active components in *S. miltiorrhiza* could be classified as lipophillic diterpene quinone pigments, generally known as tanshinones (Liao et al. 2009), and hydrophilic phenolic acids which are mainly rosmarinic acid (RA) and its derivatives lithospermic acid B (LAB) (Huang et al. 2008). When hairy root cultures of *S. miltiorrhiza* were exposed to MeJA, cryptotanshinone and tanshinone II A increased as high as 23-fold and 4.5-fold, respectively (Wang et al. 2007a), and RA and LAB approximately twice and sixfold higher as well (Xiao et al. 2009). Transcriptome analysis suggested an extensive jasmonate mediated genetic reprogramming of metabolism, which correlated well with the observed shifts in the biosynthesis of the metabolites in jasmonate-elicited *S. miltiorrhiza* hairy root cultures (Xiao et al. 2009). The coding genes of 3-hydroxy-3-methylglutaryl-CoA reductase (HMGR), 1-deoxy-D-xylulose-5-phosphate reductoisomerase (DXR) and cytidine monophosphate kinase (CMK) involved in diterpene (the precursor of tanshinones) biosynthesis pathway and 4-hydroxyphenylpyruvate reductase (HPPR), phenylalanine ammonialyase (PAL) and 4-coumarate coenzyme A ligase (4CL) in RA biosynthesis pathway were significantly induced by JAs (Liao et al. 2009; Wang et al. 2009; Xiao et al. 2009; Yan et al. 2009, 2010). Therefore, it could be assumed that endogenous JA levels by overexpression can persistently and efficiently improve the synthesis of bioactive substances in *S. miltiorrhiza*.

Most genes involved in JA biosynthesis are themselves also JA inducible (Strassner et al. 2002), in feed-forward regulation (Isayenkov et al. 2005). The biosynthesis of JA proceeds via an oxylipin pathway (Vick and Zimmerman 1984; Ziegler et al. 1997; Schaller et al. 2004) and MeJA is produced after methylation of JA (Seo et al. 2001). In JA biosynthesis pathway, the intermediate allene oxide, is unstable in vitro and can hydrolyzes non-enzymatically into α- and γ-ketols and racemic 12-oxo-phytodienoic acid (OPDA), which only amounts to 10–15 % of the total degradation products (Brash et al. 1988). However, under cellular conditions presumably most of the allene oxide is converted by allene oxide cyclase (AOC), forming exclusively the 9S, 13S enantiomer of OPDA which carries the enantiomeric structure of the naturally occurring JA (Hamberg and Fahlstadius 1990). This specificity of AOC determines the stereochemistry of the side chains in the naturally occurring jasmonate structure (Ziegler et al. 2000). Due to this fact, AOC-catalyzed step is regarded as the most critical step in JA biosynthesis. Therefore, *AOC* seems to be the potential target in regulation of metabolites biosynthetic in plant.

Here, we report the biochemical and functional characterization of a novel allene oxide cyclase from *S. miltiorrhiza*. Subsequently, *SmAOC* was overexpressed in *S. miltiorrhiza* hairy roots to investigate whether the production capacities of three active compounds (tanshinone IIA, RA and LAB) would be elevated. Otherwise, expression levels of key genes in the biosynthetic pathway of

these compounds were altered as well. This study suggested that genetic manipulation of AOC would improve the production of valuable secondary metabolites by regulating the biosynthesis of JAs in plant.

Materials and methods

Plant materials and elicitor treatments

The seedlings of *S. miltiorrhiza* were cultured on sterile MS basal medium at 25 °C under 16 h light/8 h dark photoperiod cycles in tissue culture room. To understand the role of *SmAOC* in responses to plant defense, 3-week-old seedlings were treated with three kinds of elicitors. MeJA (0.1 mM) was sprinkled on the surface of leaves slightly. Cold stress was carried out by chilling the plant in a 4 °C refrigerator. For the time-course experiment, plant templates were collected at 0, 2, 4, 6, 8, 12 and 24 h after treatments started. For UV irradiation treatment, seedlings were collected after 0.5 h of 254 nm wavelength UV exposure at an irradiance of 0.8 Wm^{-2}. Total RNA of samples were extracted for further analyses of expression profiles by real-time quantitative PCR (RT-qPCR).

RNA and DNA isolation

Total RNA was isolated by Plant RNA Isolation Mini Kit (Watson Biotechnologies, China). The genomic DNA was extracted by cetyl trimethyl ammonium bromide (CTAB)-based method (Murray and Thompson 1980). The quality and concentration of RNA and DNA samples were checked by agarose gel electrophoresis and spectrophotometry (Thermo Electron Corporation, USA). RNA samples were stored at −70 °C and DNA at −20 °C.

Molecular cloning of the *Sm*AOC

1 μg of total RNA was converted into 3′- and 5′-RACE-Ready first-strand cDNA respectively using Smart™ RACE cDNA Amplification Kit (Clontech, USA), which was used for 3′- and 5′-cDNA end amplification of *SmAOC*. Homologous primers *SmAOC*3-1 (for first PCR amplification) and *SmAOC*3-2 (for nested amplification) used for the amplification of 3′-cDNA were designed based on the conserved nucleotide sequences among the known *AOC*s from Genbank. According to the result of *SmAOC* 3′-cDNA sequencing, two gene-specific primers, *SmAOC*5-1 (as first amplification primer), *SmAOC*5-2 (as nested amplification primer) were designed for amplifying 5′-cDNA. The amplification of full-length *SmAOC* cDNA used *SmAOC*F and *SmAOC*R as primers and first-strand cDNA as the template. PCR reaction condition: 94 °C for 5 min, 35 cycles (94 °C for 30 s, 60 °C for 30 s, 72 °C for 1 min), 72 °C for 10 min. To detect whether intron(s) were present in the *SmAOC* gene corresponding to the full-length cDNA, PCR amplification was carried out using the same primers and reaction system as that for the cloning of the full-length cDNA except that the template was substituted by genomic DNA and the extension time at 72 °C was prolonged up to 3 min. The amplified PCR product was purified and cloned into pEASY-T vector and then sequenced. Gene-specific primers were listed in Table 1.

Bioinformatics analysis

The molecular information about the full-length cDNA of *SmAOC*, sequence characterization of predicted protein

Table 1 Primers used in this study

Reaction	Primer name	Sequence (5′–3′)
RACE PCR	*SmAOC*3-1	CTCGG(A/C)GATCT(T/C)GT (G/C)CC
	*SmAOC*3-2	AGCTT(T/C)TA(T/C)TTCGG (A/T/C)G(A/G)(T/C)TA(T/C)GG
	*SmAOC*5-1	GAAGTTAGCAATGGTGGCCTG
	*SmAOC*5-2	AGCTTGACCGTGCCAGACACA
	SmAOC-F	ATGGCTTTCACTAACTCCATC
	SmAOC-R	TCAATTTGTGAAGTTAGCAAT
Real-time PCR	*SmAOC* RTF	CAACTCCATCCAAGGTTCAGG
	SmAOC RTR	TCGCCGGAGTAGAGCTTGTTG
	SmCMK RTF	CCTTGGTGGTGGCAGCAGTAA
	SmCMK RTR	GGTGGAGGAATATCTTCGACG
	SmDXR RTF	TGGCCAGAGAGAATCTACTGC
	SmDXR RTR	GGCTGCACTAAGAACTCCGGT
	SmHMGR RTF	ACGTGCGTGTTGCTACGAGAC
	SmHMGR RTR	CGTCGCCAGTGCTGCAACTAA
	SmPAL RTF	ACCTACCTCGTCGCCCTATGC
	SmPAL RTR	CCACGCGGATCAAGTCCTTCT
	SmC4H RTF	CCAGGAGTCCAAATAACAGAGCC
	SmC4H RTR	GAGCCACCAAGCGTTCACCAA
	Sm4CL RTF	ATTCGCATTCGCATTTCTCGG
	Sm4CL RTR	GCGGCGTAGTGCTTCACCTTT
	SmTAT RTF	TTCAACGGCTACGCTCCAACT
	SmTAT RTR	AAACGGACAATGCTATCTCAAT
	SmHPPR RTF	GACTCCAGAAACAACCCACATT
	SmHPPR RTR	CCCAGACGACCCTCCACAAGA
	Polyubiquitin-F	ACCCTCACGGGGAAGACCATC
	Polyubiquitin-R	ACCACGGAGACGGAGGACAAG
Transgene PCR	*rol*B F	CGAGGGGATCCGATTTGCTT
	*rol*B R	GACGCCCTCCTCGCCTTCCT
	*rol*C F	TCGCCATGCCTCACCAACTCAC
	*rol*C R	CCTTGATCGAGCCGGGTGAGAA
	hpt F	CGATTTGTGTACGCCCGACAGTC
	hpt R	CGATGTAGGAGGGCGTGGATATG

was carried out on Vector NTI advance 11. Open reading frame (ORF) Finder and Genbank BLASTs were carried out on NCBI (http://www.ncbi.nlm.nih.gov). Multiple alignments of amino acid sequences were carried out using the ClustalX software (Thompson et al. 1997) against NCBI deposited sequences of *Sm*AOC (boxed) and other AOCs. Phylogenetic tree was constructed by the neighbor-joining method (Saitou and Nei 1987) with MEGA2.1 program (Kumar et al. 2001) based on the amino acid sequences alignment established by ClustalX. The numbers on the branches represent bootstrap support for 1,000 replicates. The chloroplast transit peptide (cTP) of *Sm*AOC was predicted on the website (http://www.cbs.dtu.dk/services/ChloroP). *AOC*s used for bioinformatics analysis were listed in Table 2.

Expression of recombinant *Sm*AOC in *Escherichia coli*

The cDNA of *SmAOC* was inserted between the *Bam*HI and *Sac*I restriction sites of pET32a vector. The constructed plasmid pET32a-*SmAOC* was introduced into *E. coli* strain BL21(DE3). The transformed stain was cultured in 250 mL of Luria–Bertani (LB) medium containing 100 mg/L carbenicillin at 37 °C till reached OD_{600} value about 0.5. Isopropyl thiob-D-galactoside (IPTG) was added to a final concentration of 1 mM to induce the expression of target protein, and then a further incubation at 37 °C for 0, 1, 2 and 3 h. BL21 strain containing empty pET-32a vector with or without 3 h IPTG induction were used as controls. The bacteria were pelleted, subjected to two freeze–thaw cycles, and lysed by sonication in 20 mM Tris–Cl, 10 % glycerol, 0.1 % Tween 20, and 0.5 M NaCl at pH 7.5. The extracts from bacteria were separated by SDS-PAGE and stained with Coomassie blue.

Table 2 *AOC*s used for bioinformatics analysis

Name	Species	Accession no.
*AtAOC*1	*Arabidopsis thaliana*	NM113475
*AtAOC*2	*Arabidopsis thaliana*	NM113476
*AtAOC*3	*Arabidopsis thaliana*	NM113477
*AtAOC*4	*Arabidopsis thaliana*	NM101199
CaAOC	*Camptotheca acuminata*	AY863428
HlAOC	*Humulus lupulus*	AY687338
HnAOC	*Hyoscyamus niger*	AY708383
HvAOC	*Hordeum vulgare*	AJ308488
PhAOC	*Oryza sativa*	EU090802
OsAOC	*Petunia hybrida*	EU652410
PpAOC	*Physcomitrella patens*	AY154776
PsAOC	*Pisum sativum*	AB095986
StAOC	*Solanum tuberosum*	AY135641
VvAOC	*Vitis vinifera cultivar Riesling*	DQ406694
ZmAOC	*Zea mays*	EU967124

Tolerance against salt stress in bacteria

The pET32a-*SmAOC* transformant was induced by 1 mM IPTG for 2 h. Two negative controls, pET32a-*SmAOC* transformant without IPTG inducing and BL21(DE3) *E. coli* strain harboring empty vector with IPTG inducing were cultured under the same condition. Subsequently, diluted these three strains (equal OD_{600} value) to 10^{-2}, 10^{-3}, 10^{-4}-folds respectively. After that, 10 μL of each sample was separately dipped onto two plates of LB agar medium containing 100 mg/L carbenicillin with low concentrations (0.08 M) or high concentration (0.4 M) NaCl. The plates were incubated at 37 °C for 24 h (with 0.08 M NaCl) or 48 h (with 0.4 M NaCl), since bacteria grew more slowly under higher concentration salty condition.

Real-time quantitative PCR assays

The transcript abundance of objective genes in organ tissue, treated samples and transgenic hairy root cultures were analyzed by RT-qPCR. Total RNA was extracted from various organs including roots, stems and leaves, respectively. For inducible study, RNA was isolated after treatment for different periods. For transgenic analysis, RNA was isolated from the 6 weeks liquid hairy roots culture. First-strand cDNA samples were synthesized from the isolated total RNA by following the instruction of Transcript First-Strand cDNA Synthesis SuperMix kit (TransGen Biotech, China). RT-qPCR was performed on Thermal Cycler Dice™ Real-Time System Machines (TaKaRa, Japan) with the SYBR Premix Ex Taq™ II Perfect Real-Time kit (TaKaRa, Japan) according to manufacturer's instruction. Partial of *polyubiquitin* gene (Xiao et al. 2009) was amplified as reference. Gene-specific primers were listed in Table 1. The relative mRNA level was calculated as $2^{-\Delta\Delta Ct}$ method (Livak and Schmittgen 2001) and the value of roots, 0 h or wild-type hairy root was normalized to "1.0".

Construction of plant expression vectors and hairy root cultivation

The *SmAOC* cDNA was inserted into the *Nco*I and *Spe*I sites in pCAMBIA1304 (CAMBIA, Canberra, Australia) containing hygromycin phosphotransferase gene (*hpt*) to generate the plant expression vector p1304-*SmAOC*, then was transformed into *Agrobacterium rhizogenes* strain C58C1 which was used for establishing *S. miltiorrhiza* hairy root culture. Wild type (WT) and blank vector (BV) transformed hairy root lines were established and used as

blank control and vector control. Hygromycin-resistance gene *hpt* was used as a selectable marker in eukaryotic expression vector due to its phosphorylation and inactivation of hygromycin. When the transgenic hairy roots were 2–4 cm in length on half-strength B5 (1/2 B5) solid medium, they were selected by 10 mg/L hygromycin. Then, the hygromycin-resistant lines were transferred into 1/2 B5 liquid medium and kept in an orbital shaker at 100 rpm and 25 °C in the dark.

PCR identification of transgenic hairy roots

Total genomic DNA was isolated from transgenic and control hairy roots and used as a template for PCR analysis to detect the presence of *Agrobacterium rol* (*B*, *C*), selectable marker *hpt* and transformed *SmAOC* in transgenic hairy roots. To eliminate the interference from endogenous genes, forward and reverse primers for the integration confirmation of *SmAOC* into the transformed hairy root genome were designed to cover the *SmAOC* sequence and the vector sequence. The *Agrobacterium* carrying p1304-*SmAOC* was used as a positive control. The primers for gene detection were listed in Table 1.

Compound extraction and analysis

After 45 days of culture in liquid medium, the hygromycin selecting and PCR testing positive transgenic strains and control hairy roots were harvested. 3 WT control lines, 3 BV independent clones and 5 typical transgenic hairy roots were subjected to further examination. The hairy roots were dried at 60 °C for 12 h to constant dry weight and powdered to a homogeneous size by a mill, sieved through a No. 100 mesh. Extraction of compounds (tanshinone IIA, RA and LAB) was based on the method described by Zhu et al. (2007). 0.3 g powder sample was extracted for 30 min by sonication in 70 % methanol and then centrifuged at 9,000 rpm for 5 min. The extraction volume was 25 mL and the weight loss was made up with 70 % methanol after extraction. The sample solution was filtered through a 0.2 μm organic membrane for injection. LC–MS/MS analysis followed Xiao et al. (2009) method with minor modifications. RA and LAB were quantitated in multiple reactions monitoring (MRM) mode and the selected transitions of *m/z* were 359 → 61 and 717 → 519, while tanshinone IIA was in selected ion monitoring (SIM) mode and 295 *m/z* was selected as detecting ion.

Statistical analysis

Each result shown in figures was the mean of at least three replicated treatments and the SD value was calculated. Data for WT and BV were the means of three independent strains. All results were analyzed by single factor ANOVA and means were separated by LSD test at the 5 % level of significance using Statgraphics Plus 5.

Results and discussion

Cloning and bioinformatics analysis of *Sm*AOC

A novel *AOC* from *S. miltiorrhiza* has been identified in this study by RACE method. The full-length *SmAOC* cDNA was 910 bp (Genbank No.: HM156740) with an ORF of 738 bp. The comparison between cDNA and genomic DNA sequence of *SmAOC* revealed that a 123 bp intron was present in the genomic DNA (Fig. 1). The deduced *Sm*AOC protein contained 245 amino acid residues with a predicted molecular mass of 26.795 kDa. Inspection of *N*-terminal amino acid sequence revealed *Sm*AOC carried a chloroplast transit peptide and the predicted cleavage site lied between the 47th and 48th amino acids (Fig. 1). In previous studies, AOC protein as well as the preceding enzymes in octadecanoid biosynthesis, lipoxygenase (LOX) and allene oxide synthase (AOS), had been reported to localize in the chloroplasts (Schaller 2001;

```
                                                        ggtctcgaggctttcatcattt
  1 atggctttcactaactccatcactcccaaggctgaagcaccttctgctctcccatccacc
    M  A  F  T  N  S  I  T  P  K  A  E  A  P  S  A  L  P  S  T
 61 ggaaatcggatcgccgatcttcgtttctcgacctccgtttcaaccaaaatttgcaatact
    G  N  R  I  A  D  L  R  F  S  T  S  V  S  T  K  I  C  N  T
121 ccgaatcggagatcgatttcctgcgccagatcttccaagccgcaagccttcttcggcctc
    P  N  R  R  S  I  S↓C  A  R  S  S  K  P  Q  A  F  F  G  L
181 tggagcaaacccaagccggagccttcaactccat----gtaagaataacctagattgtaa
    W  S  K  P  K  P  E  P  S  T  P  S ----------intron---------
    gaataacctagatttctctttgattttgttgaattgattacgcgttggaagcagatctgt
    ------------------------ intron ----------------------------
    gatcaattctcagcaaactgatccgcagcgttaatttcag---------ccaaggttcag
    ---------------------- intron ----------------------  K  V  Q
226 gagctgtacgtgtacgagatgaacgagcgcgaccgcggcagcccggcctacctacggctg
    E  L  Y  V  Y  E  M  N  E  R  D  R  G  S  P  A  Y  L  R  L
286 agccagaaggagcagaacaccctgggcgacctcgtccccttctccaacaagctctactcc
    S  Q  K  E  Q  N  T  L  G  D  L  V  P  F  S  N  K  L  Y  S
346 ggcgacctgcagaagagattgggcatcacggccggtctctgcgtgctcatccagcacttt
    G  D  L  Q  K  R  L  G  I  T  A  G  L  C  V  L  I  Q  H  F
406 cccgaccagaatgccgaccgctacgaggccatctacagcttctatttcggcgattacggc
    P  D  Q  N  A  D  R  Y  E  A  I  Y  S  F  Y  F  G  D  Y  G
466 cacatctcggtgcagggcgcgtacctcacacgctccgacacttacctggccgtcaccggc
    H  I  S  V  Q  G  A  Y  L  T  R  S  D  T  Y  L  A  V  T  G
526 ggctccggcgtctttgagggtgtgtctggcacggtcaagctgcagcagatagtgttcccg
    G  S  G  V  F  E  G  V  S  G  T  V  K  L  Q  Q  I  V  F  P
586 tttaagctcttctacacgttttatttgaaggggatcaaggatttgccggcggagctggtg
    F  K  L  F  Y  T  F  Y  L  K  G  I  K  D  L  P  A  E  L  V
646 gtcaccccggtggcgccgtcgccctccgtcgagccgtcgccggctgccaaggccaccgag
    V  T  P  V  A  P  S  P  S  V  E  P  S  P  A  A  K  A  T  E
706 cctcagccaccattgctaacttcacaaat 735 tgatgtttgtagtcggaattacattt
    P  Q  P  P  L  L  T  S  Q  I      *
    tgtggtgttggtaattagctgaggtttttgttgtagtatggttattggaatttgttgcgc
    attcattcacgttttataatttatgtgattttatctcaaaaaaaaaaaaaaaaaaaaaa
    aaaaaaa
```

Fig. 1 Nucleotide sequence of *SmAOC* (contains a 123 bp intron) and the deduced amino acid sequence of the encoded protein. The *arrow* indicates the cleavage site of the deduced chloroplast transit peptide between S_{47} and C_{48}

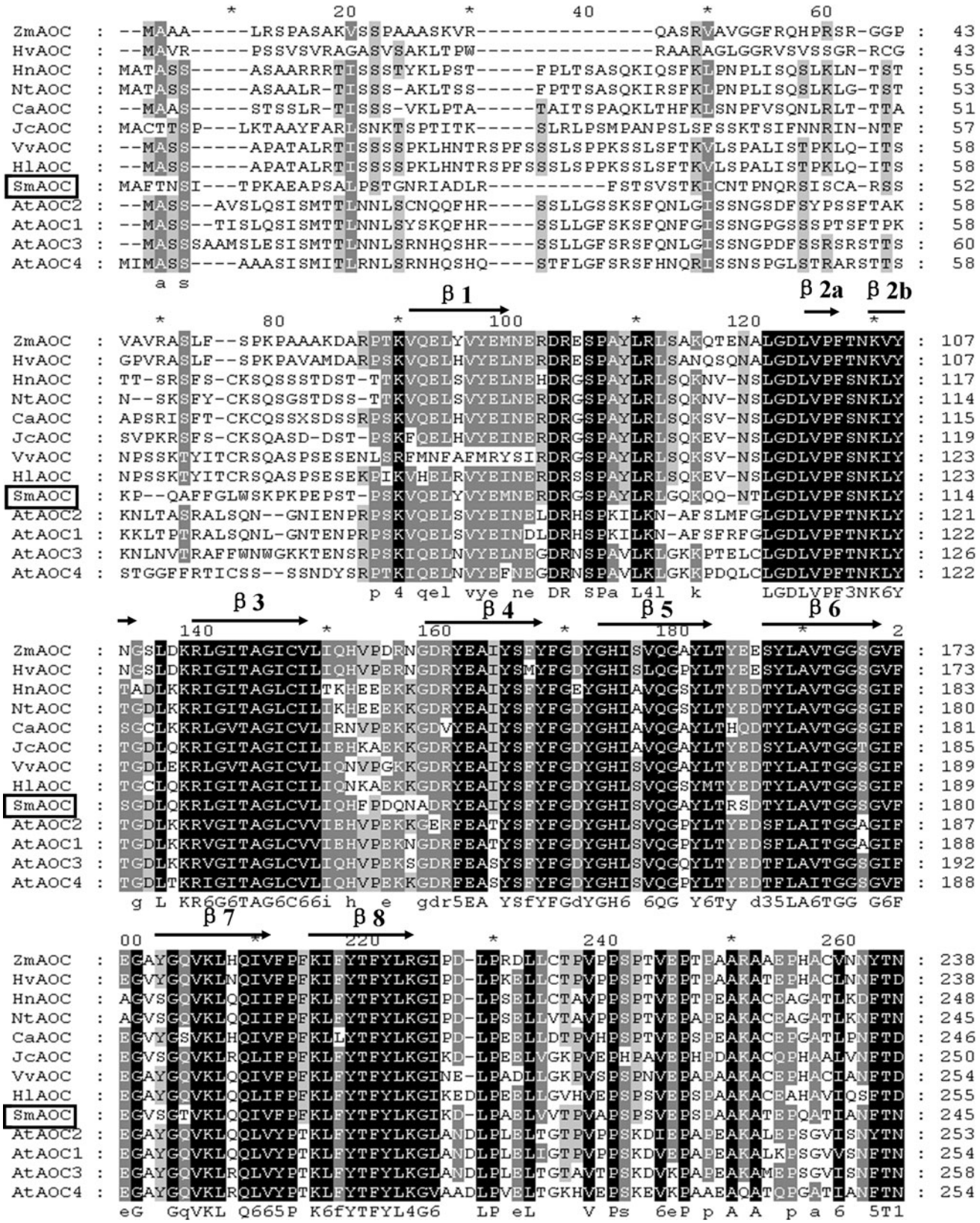

Fig. 2 Multi-alignment of amino acid sequences of *Sm*AOC (*box*) and other AOCs. The identical amino acids are showed in *white with black background* and the conserved amino acids are showed in *white with gray background*. The eight *β*-strand residues corresponding to *At*AOC2 are indicated with *horizontal arrows*. The aligned AOCs are listed in Table 2

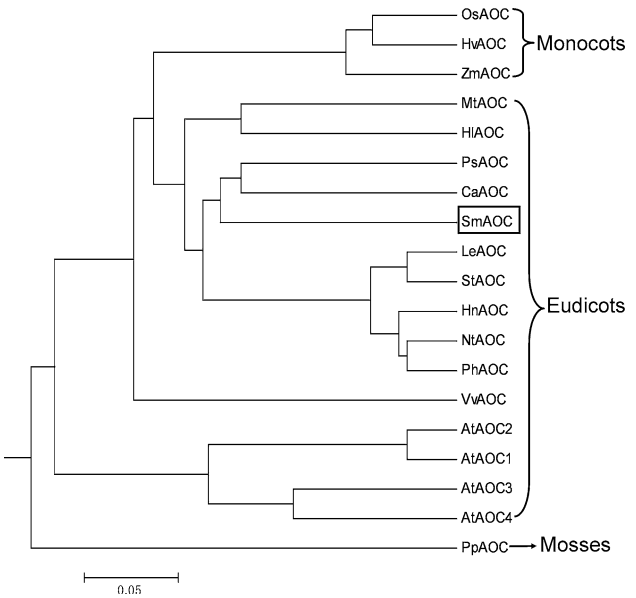

Fig. 3 Phylogenetic tree analysis of some plant AOCs proteins. Phylogenetic tree was constructed with MEGA program based on amino acid sequences alignment established by ClustalX. The *bars* represent evolutionary distance. The reliability of the tree is measured by bootstrap analysis with 1,000 replicates. The *Sm*AOC (*boxed*) clustered together with other AOCs from eudicots. Among these eudicots, *Sm*AOC was grouped in an isolated branch. The AOCs of *A. thaliana* (*At*AOC 1–4) fell into their own subgroup. The monocotyledonous AOCs were grouped in a clearly different branch. The AOCs used in phylogenetic tree analysis are listed in Table 2

Ziegler et al. 2000) and our result indicated *Sm*AOC was localized to chloroplasts too. The amino sequence of *Sm*AOC was 78, 76, 73, 72 and 71 % identical to *Zm*AOC from *Zea mays*, *Hv*AOC from *Hordeum vulgare*, *Vv*AOC from *Vitis vinifera*, *Ca*AOC from *Camptotheca acuminata* and *Hl*AOC from *Humulus lupulus*, respectively. The alignment of AOCs showed high degree of conservation in the functional region (aa 60 to the *C*-terminal), especially in the residues corresponding to the eight β-Strands of *Arabidopsis thaliana* AOC2 (Hofmann et al. 2006), rather than in the transit peptide portion (Fig. 2), but their contribution to AOC catalysis was unknown yet (the function of the region was unknown). The motifs might play an important role in the biological functions and thus were preserved in evolution, while some variations on un-conserved domain could form the molecular foundation for the diversity of AOCs' structures and functions (Jiang et al. 2008). It would be interesting to establish the importance of both motifs and their species-specific variations on the catalytic properties of AOC. The phylogenetic tree showed *Sm*AOC clustered together with other AOCs from eudicots. The result was consistent with the category of *S. miltiorrhiza* (Fig. 3). All of the bioinformatics analysis results strongly suggested that *Sm*AOC was a plant AOC protein involved in jasmonic acid biosynthesis.

Expression of recombinant *Sm*AOC and tolerance against salinity in *E. coli*

The accumulation of recombinant protein pET32a-*Sm*AOC was induced by IPTG in *E. coli.* SDS-PAGE revealed a prominent band of 45 kDa which was absent in control bacteria harboring empty vector without (lane 1) and with (lane 2) inducing (Fig. 4). It indicated that the recombinant pET32a-*Sm*AOC was about 45 kDa in molecular weight. The recombinant protein was expressed in a soluble fusion protein form containing *Sm*AOC and tag protein which was present in pET32a vector itself used for signing expressed recombinant protein. The molecular mass of tag protein showed in lane 2 was approximately18 kDa. This molecular mass coincided with pET32a vector instruction. Thus, the molecular mass of the protein encoded by the cDNA of *Sm*AOC (deduced by SDS-PAGE) was about 27 kDa, which was in agreement with the bioinformatics predicted value (26.795 kDa).

It was reported that expression of AOC in *E. coli*, yeast, tobacco (Yamada et al. 2002), *Camptotheca acuminata* (Pi et al. 2009) and *Jatropha curcas* (Liu et al. 2010) all displayed enhanced salt tolerance. In order to investigate if *Sm*AOC possessed the similar property, the salt tolerance of the transformant was tested with the spot test (Fig. 5). A strain expressed *Sm*AOC protein and two negative controls were incubated on medium with low NaCl concentration in 0.08 M and high concentration in 0.4 M. The *E. coli* strains were serially diluted 1:10 for the purpose of macroscopic cell densities. As shown in Fig. 5, strain in Row A grew well on both 0.08 and 0.4 M NaCl agar plates; the growth of strain in Row B was inhibited on 0.4 M NaCl obviously than on 0.08 M NaCl; strain in Row C also grew poorly in the presence of 0.4 M NaCl. The culture of

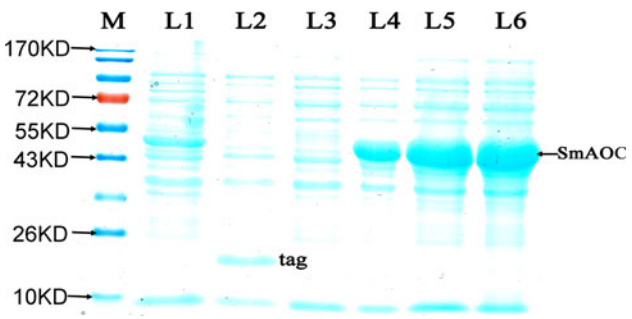

Fig. 4 SDS-PAGE analysis of the recombinant *Sm*AOC protein expressed in *E. coli* BL21 (DE3). *Lane M* protein marker, *lane 1* uninduced pET-32a as control, *lane 2* induced pET-32a for 3 h with a 18 kDa tag protein, *lane 3–6*, pET-32a-*Sm*AOC induced by 1 mM IPTG for 0, 1, 2 and 3 h, respectively. *Arrow* shows the molecular mass of recombinant protein pET-32a-SmAOC (tag protein plus SmAOC protein) is approximately 45 kDa. It conforms the molecular mass of the *SmAOC* protein is consistent with the predicted value (about 27 kDa)

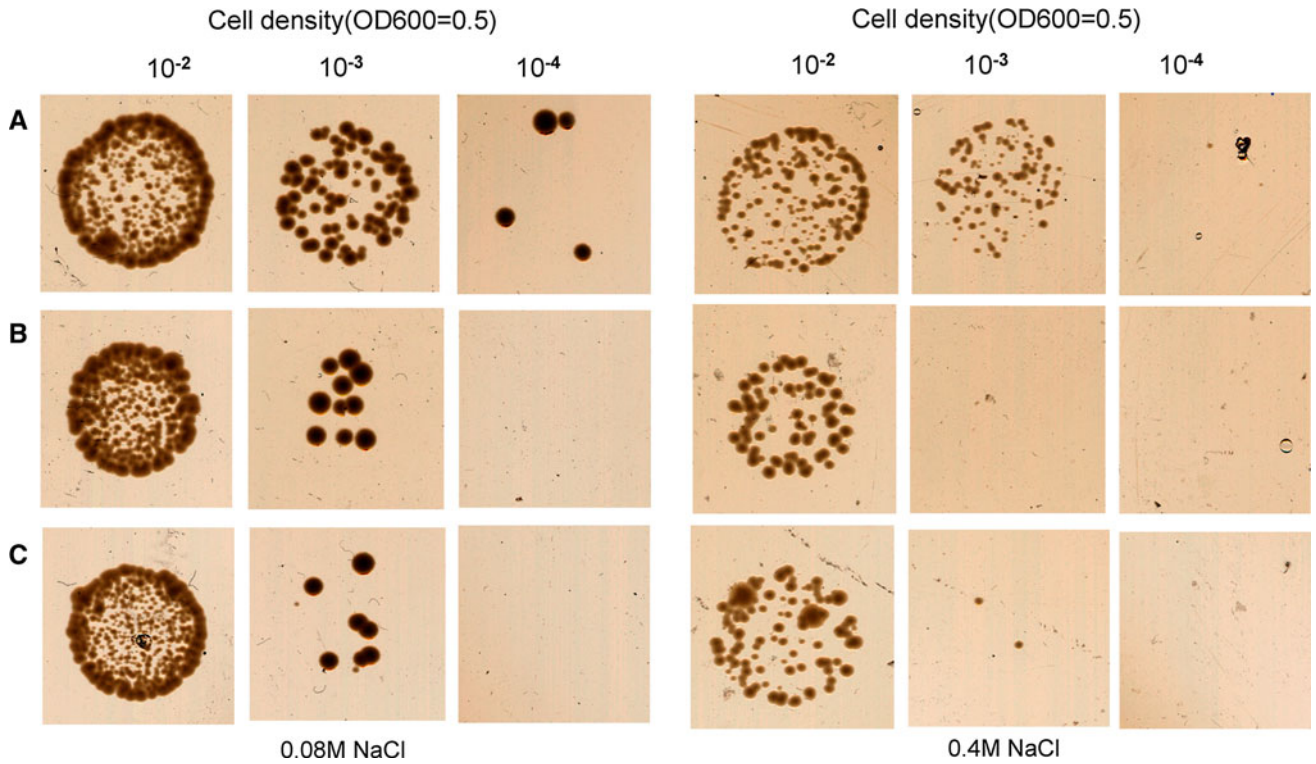

Fig. 5 Effect of salt concentration (0.08 or 0.4 M NaCl) on the growth of transformed *E. coli* cells. *Row A* recombinant pET32a-*Sm*AOC induced by IPTG, *row B* recombinant pET32a-*Sm*AOC without IPTG inducing, *row C* bacteria harboring empty vector with IPTG inducing. Serial dilutions, 1:10, were made from these *E. coli* transformants, and were spotted equally on LB agar plates

different cell density showed same tendency. In the high salt concentration plate, 10^{-3} and 10^{-4} diluent control bacteria could hardly survive, while the growth of engineered strain was not obviously impacted. This result indicated that *Sm*AOC expressed *E. coli* strains promoted the salt tolerance as previous reports. Since *E. coli* did not contain JAs biosynthetic pathway, these results revealed a potential property of AOCs other than catalyzing JA biosynthesis.

Tissue-specific and induced expression profile of *Sm*AOC

The transcription of *SmAOC* could be detected in all tested tissues of *S. miltiorrhiza* with the strongest expression in leaves and lower in stems and roots (Fig. 6a). The result suggested *SmAOC* was a constitutive expressed gene and the pattern was similar to that of *AOC* gene in *A. thaliana* (Stenzel et al. 2003b) and *J. curcas* (Liu et al. 2010). Moreover, tissues with high JA levels had high levels of *AOS* transcripts in barley as well (Maucher et al. 2000). It indicated that the expression of the genes on JA biosynthesis pathway has been strongly correlated with JA contents.

Abiotic elicitors such as MeJA and stress conditions such as UV and low temperature exhibited a remarkable effect on the production of secondary metabolites involved in plant defense system. Many studies had been carried out to investigate expression profiles of JAs biosynthesis genes under elicitor treatments (Jiang et al. 2008; Pi et al. 2009), which will be helpful to uncover molecular induction mechanism for further JAs biosynthesis engineering in plant.

Under the 0.1 mM MeJA induction, as shown in Fig. 6b, *SmAOC* expression was rapidly and strongly induced and reaching the peak at 2 h (6-fold of original value) followed by a gradual decrease at 4–6 h (3.7–2.5 folds). Interestingly, the expression level of *SmAOC* increased again at 8 h (4.25-folds), then went back to the beginning level after 24 h. This observation is according with *AOS* expression pattern in tobacco (Ziegler et al. 2001). A positive feedback regulatory system of JA biosynthesis was reported that activity of JA biosynthesis enzymes promoted by JA treatment (Sasaki et al. 2001), and the whole JA biosynthesis pathway are JA inducible (Wasternack 2007). Thus, the subsequent increasing of *AOC* expression at 8 h was caused by the endogenously synthesized JA which improved by the pervious induction of MeJA.

UV exposure induces oxidative stress in plants, so JA response might also be involved in the defense against UV irradiation. To investigate how *SmAOC* response to UV, the expression of *SmAOC* was detected after irradiation of 30′ by UV of 254 nm. The expression level of *SmAOC* provisionally presented a minor increase at 2 h (1.4-fold of

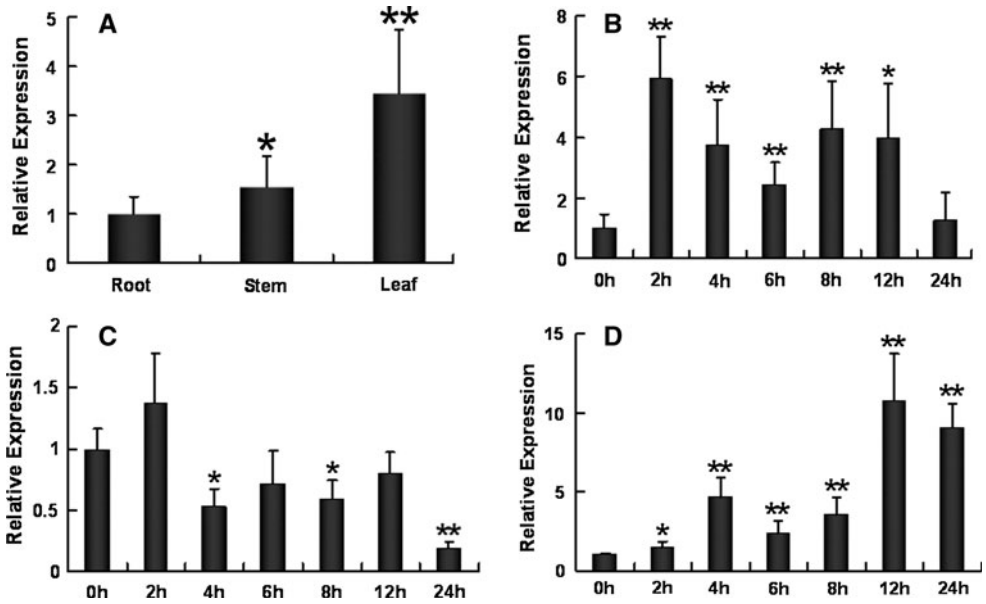

Fig. 6 Tissue-specific and induce expression profile of *SmAOC*. **a** Expression pattern of *SmAOC* in different *S. miltiorrhiza* tissues. Expression profile analysis of *SmAOC* under different treatments (**b** 0.1 mM MeJA, c UV, **d** low temperature 4 °C) for seven different periods of time (0, 2, 4, 6, 8, 12, and 24 h) followed by RT-qPCR analysis. The value of root or 0 h is normalized to "1.0". The results represent mean ± standard deviation ($n = 3$). *Asterisks* indicate statistically significant differences of transgenic lines when compared with the control line 0 h (*$p < 0.05$; **$p < 0.01$)

0 h control), then fleetly dropped down to the level lower than origination till 24 h (Fig. 6c), even the expression at 24 h faded to only a quarter of that at 0 h. This profile was different from AOC in *Hyoscyamus niger* (Jiang et al. 2008). Under UV treatment, although the *Hn*AOC expression level slightly increased and reverted to the original level in 2–5 h, it was not inhibited as *Sm*AOC. This inconsistency indicated that there should be a different regulation mechanism of UV in various species.

Cold stress has been shown to induce transient Ca^{2+}, influx into the cell cytoplasm (Knight 1999; Sanders et al. 1999). Under the condition of low temperature, the transcript of *SmAOC* increased gently (2- to 4-folds) before 8 h, but continued to increase markedly and obviously (almost 10-folds, $p < 0.01$) at 12–24 h (Fig. 6d). In the present study, the peak of *Sm*AOC mRNA accumulation occurred at 2 h in response to all the treatments except for low temperature (Fig. 6). However, the low temperature activated *Sm*AOC expression distinctly and the effects lasted for a longer time than other treatments. We supposed that the process was slowed down in low temperature. The results above revealed that *SmAOC* was a stress-responsive gene and could be effectively elicited at least at transcription level, although its expression responded at different levels and in different profiles to various treatments. These stresses induced expression profiling of *SmAOC* might demonstrate the possible resistance mechanism regulated by JA signaling in plant cell.

In vivo functional characterization of *SmAOC*

To investigate the global function of *SmAOC in vivo*, *SmAOC* overexpressed transgenic hairy root cultures were obtained after PCR identification. Morphology and growth of the selected transgenic lines were statistically insignificant from those of wild-type hairy roots. Then, LC–MS/MS analysis was performed to measure the contents of tanshinone IIA, RA and LAB in both control and transgenic hairy root lines. The production of three components was not diverse obviously between WT and BV control lines ($p > 0.1$), suggesting that vector pCAMBIA1304 hardly interfered with transgenic strategy. Compared with the control hairy root lines (WT and BV), the accumulation of tanshinone IIA was significantly increased in all transgenic lines. The best clone (T7) produced tanshinone IIA over 15-folds (0.56 mg/g) more than the basal level of controls (0.037 and 0.035 mg/g in the WT and BV lines, respectively). However, tanshinone IIA production was highly variable among the five independent transgenic hairy roots, ranging from 0.059 to 0.56 mg/g dry weight (DW), which is about 1.6- to 15.1-fold of that of WT (Fig. 7). *SmAOC-ovx* also increased phenolic acids production. The highest amount of RA was observed in transgenic line T1 (2.8 mg/g DW), which is 2.1-folds of that in WT (1.3 mg/g DW). Furthermore, T1 accumulated LAB at about 19.0 mg/g DW on a dry weight basis, which was 1.8-fold of WT (10.7 mg/g DW) and 2.3-fold of BV (8.1 mg/g DW) (Fig. 7). Nevertheless, the disparity of the phenolic acids amounts between transgenic lines and control lines was not as great as that of tanshinone. The difference between this two disparity illustrated overexpression of *SmAOC* had different influence on regulating the biosynthesis pathways of these two kinds of compounds. Transgenic *SmAOC* engineering generated more notable effect on the accumulation of fat-soluble tanshinone than water-soluble phenolic acids.

It was validated that JAs could activate multiple secondary metabolite pathways. JAs could induce pathways synthesizing components of a wide structural variety,

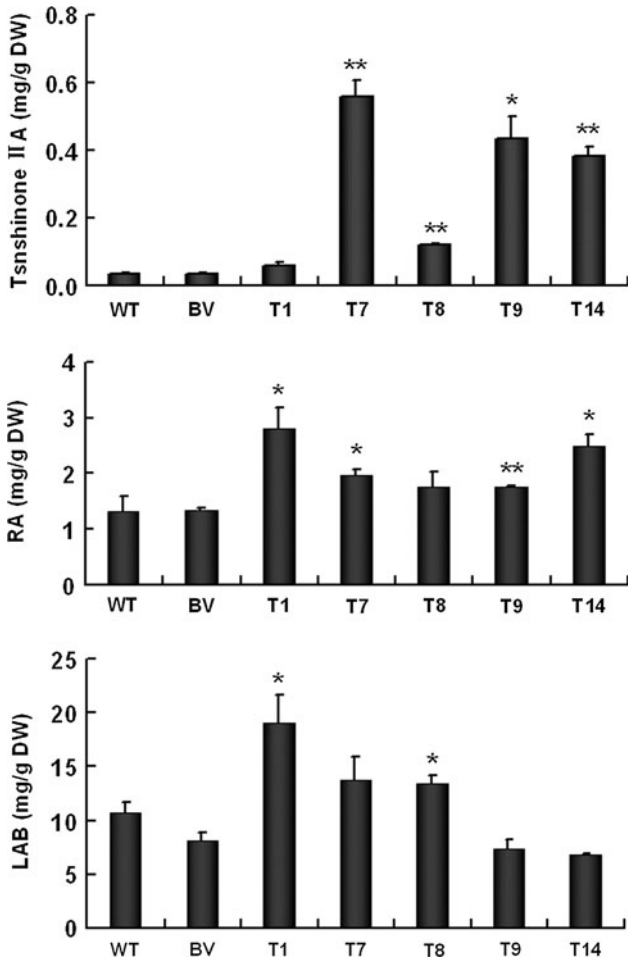

Fig. 7 Compounds contents analysis. WT wild-type hairy root, BV hairy root transformed with blank vector. T1–T14 are transgenic hairy root lines. *Vertical bars* represent standard deviation. The amounts of WT and BV are the average of triplicate samples. The values are mean ± SD of triplicate analyses. *Asterisks* indicate statistically significant differences of transgenic lines when compared with the control line WT (*$p < 0.05$; **$p < 0.01$)

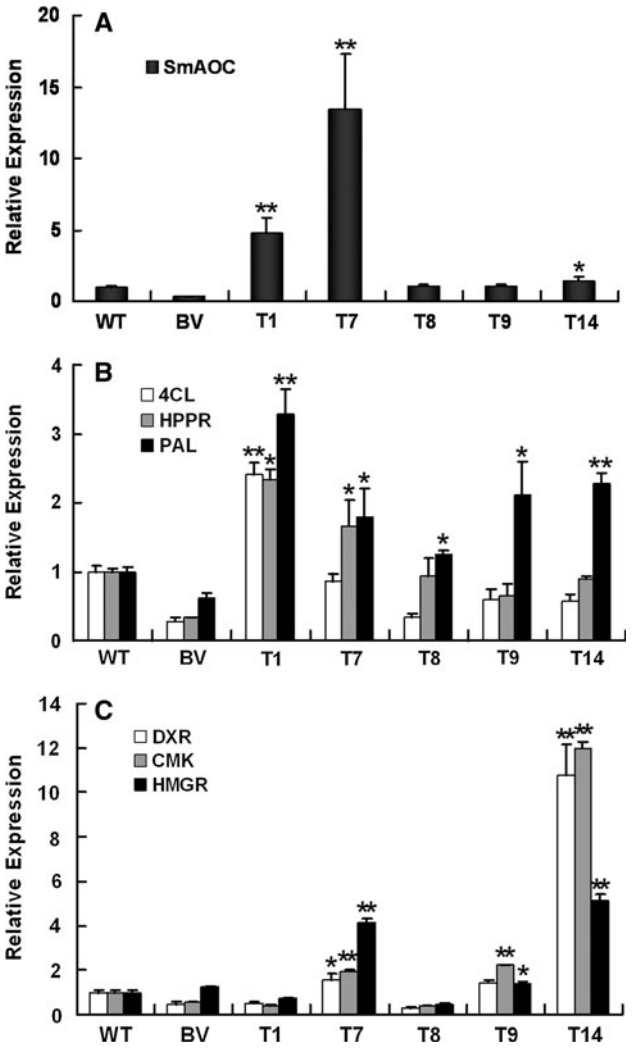

Fig. 8 RT-qPCR analysis of *SmAOC* and the terpenoids and RA biosynthesis genes in hairy root lines. **a** The relative expression level of *SmAOC*, **b** the relative expression level of RA biosynthesis genes 4*CL*, *HPPR* and *PAL*, **c** the relative expression level of terpenoids biosynthesis genes *DXR*, *CMK* and *HMGR*. *WT* wild-type hairy root, *BV* hairy root transformed with blank vector. *T1–T14* are transgenic hairy root lines. *Vertical bars* represent standard deviation. The value of WT is normalized to "1.0". The results represent mean ± standard deviation ($n = 3$). *Asterisks* indicate statistically significant differences of transgenic lines compared with the control line WT (*$p < 0.05$; **$p < 0.01$)

encompassing multiple branches of the important secondary metabolite classes, such as phenylpropanoids, alkaloids and terpenoids (Zhao et al. 2005). In preceding reports, exposed to 0.1 mM methyl jasmonate, tanshinone IIA was 4.5-fold higher than that of the control (Wang et al. 2007b), while RA and LAB accumulation enhanced to about twice and sixfold of dry weight, respectively (Xiao et al. 2009) in *S. miltiorrhiza* hairy root cultures. Similar results were observed in our work. This demonstrated that engineering of jasmonate biosynthesis had similar effect as exogenous JAs. Furthermore, sequentially secondary metabolites accumulation in *S. miltiorrhiza* was achieved.

Expression analyses of correlative biosynthetic genes

To investigate the expression level of the introduced *AOC* gene, total RNA was isolated from the generated hairy root lines and measured by RT-qPCR. It was observed that *SmAOC* was successfully overexpressed in all transgenic root lines (Fig. 8a). The highest 12-fold increase of *SmAOC* expression level emerged in transgenic cultures line T7 when compared with WT line. And in the other four transgenic lines, the relative expression of *AOC* was 10 % to threefold higher than that in WT control. It had been suggested that JA biosynthesis was regulated by a positive feedback, since all genes encoding enzymes of JA biosynthesis were JA-inducible (Wasternack 2007). Nevertheless, the different expression levels of *SmAOC* among separated

transgenic lines might be due to the effects of insertion sites where the introduced gene was integrated into hairy roots genome or other unknown reasons. Overexpression procedure increased *AOC* transcription in the transgenic hairy roots, but increases in secondary metabolites accumulation were not markedly consistent. This might be caused by the subtle and complex regulating process of phytohormone JAs to secondary metabolism network.

Prior reports indicated that an extensive genetic reprogramming of metabolism correlated with the observed shifts in the biosynthesis of the metabolites investigated in JA-elicited cell suspension cultures, such as *Medicago truncatula* (Suzuki et al. 2005) and *Arabidopsis* (Pauwels et al. 2008). To better understand the relationship between secondary metabolites accumulation and their biosynthesis-related gene expression in transgenic hairy root lines, the expression of genes involved in tanshinone and RA biosynthesis pathway were measured by RT-qPCR. The results showed expression levels of *HPPR, PAL* and *4CL* in phenolic acids biosynthesis pathway (Fig. 8b), *DXR*, *HMGR* and *CMK* in terpenoid synthesis pathway (Fig. 8c) were enhanced. Compared to the WT, *PAL* gene was strongly expressed in all the transgenic lines. *4CL* and *HPPR* expression was only higher in T1 and T7 (Fig. 8b). Intriguingly, RA amounts increased in all the transgenic lines, and LAB content was boosted in T1 and T7 as well. It seems that *PAL* plays an important role in RA catalysis, which would prompt JAs-based metabolic engineering causes more significant regulation to *PAL* than other genes in *S. miltiorrhiza*. Meanwhile, both *4CL* and *HPPR* transcription were coincident with LAB accumulations, suggesting that they probably linked with LAB biosynthesis. The expression of the terpenoid synthesis pathway genes (*DXR, HMGR* and *CMK*) all showed significant differences in expression between T7, T9, T14 and control lines (WT and BV), but only minor expression variations in T1 and T8 (Fig. 8c). Accordingly, T1 and T8 contained less tanshinone II A as compared to T7, T9 and T14. These results clearly showed that *SmAOC-ovx* can activate these representative compounds biosynthesis pathways genes and then enhance the yield of target compounds. However, the amounts of metabolites in different transgenic lines (Fig. 7) were not generally proportional to the expression levels of their biosynthesis genes (Fig. 8), possibly due to additional complexity of secondary metabolites biosynthesis. The different profiles of regulated biosynthetic genes transcript between terpenoid (tanshinone IIA) and phenolic acids (RA and LAB) in *S. miltiorrhiza* transgenic lines demonstrated that different secondary metabolic pathways might obey different regulatory modules.

It appears that the expression of biosynthesis-related genes correlates with metabolites production to some degree and it may be associated with *AOC* overexpression. Many pioneering reports established most transgenic plants overexpressing JA biosynthetic pathway genes failed to increase basal level of JAs, but presented higher and earlier accumulation of JAs upon stresses (Laudert et al. 2000; Stenzel et al. 2003a). Transgenic *Arabidopsis* overexpressing jasmonic acid carboxyl methyltransferase (JMT) had a threefold elevated level of endogenous methyl jasmonate without altering JA content and the transgenic plants exhibited constitutive expression of jasmonate-responsive genes (Seo et al. 2001). Overexpression of AOS did not increase JA levels in healthy tobacco, but promoted the wound-induced accumulation of JA in transgenic lines (Wang et al. 1999). A possible explanation of this inconsistency is that the synthesis and consumption of JA have been achieved dynamic equilibrium. In other words, overexpressing JA biosynthetic genes could increase JA synthetic velocity, but its releasing velocity was also enhanced due to its hormone characteristic, thus the absolute value of instantaneous JA amount displayed no boost.

In conclusion, with the long-term aim of potentially modifying the endogenous levels of JA in *S. miltiorrhiza* by gene transfer and then investigating the crosstalk between JA signaling and secondary metabolism network, we describe in this paper the molecular cloning of a *S. miltiorrhiza* allene oxide cyclase cDNA and the characteristic of *SmAOC-ovx* hairy roots. Although it was observed that not all the transgenic lines exhibited the same capacity in producing metabolites, the target compounds levels in *SmAOC* transgenic lines were almost higher than controls. Furthermore, as compared to enhancing single or several steps of the pathway, engineering jasmonate biosynthesis may be a more efficient strategy in globally modulating the production of target compounds especially if the biosynthesis pathway is unknown. Moreover, overproduction of endogenetic jasmonates in transgenic lines may lead to more sequential accumulation of the corresponding metabolites compared to exogenous treatment. The present study provides a desirable candidate gene resource to increase the content of valuable natural products via appropriate JA pathway genetic engineering.

Acknowledgments This work was supported by grants from National Natural Science Foundation of China (30900786, 31100221 and 31160059).

References

Brash AR, Baertschi SW, Ingram CD, Harris TM (1988) Isolation and characterization of natural allene oxides: unstable intermediates in the metabolism of lipid hydroperoxides. Proc Natl Acad Sci USA 85:3382–3386

Chehab EW, Braam J (2012) Jasmonates in plant defense responses. In: Witzany G, Baluška F (eds) Signaling and communication in plants, vol 14, Springer, Berlin, pp 67–88

De Geyter N, Gholami A, Goormachtig S, Goossens A (2012) Transcriptional machineries in jasmonate-elicited plant secondary metabolism. Trends Plant Sci 17:349–359

Hamberg M, Fahlstadius P (1990) Allene oxide cyclase: a new enzyme in plant lipid metabolism. Arch Biochem Biophys 276:518–526

Hayashi H, Huang P, Inoue K (2003) Up-regulation of soyasaponin biosynthesis by methyl jasmonate in cultured cells of *Glycyrrhiza glabra*. Plant Cell Physiol 44:404–411

Hofmann E, Zerbe P, Schaller F (2006) The crystal structure of *Arabidopsis thaliana* allene oxide cyclase: insights into the oxylipin cyclization reaction. Plant Cell Online 18:3201–3217

Huang B, Duan Y, Yi B, Sun L, Lu B, Yu X, Sun H, Zhang H, Chen W (2008) Characterization and expression profiling of cinnamate 4-hydroxylase gene from *Salvia miltiorrhiza* in rosmarinic acid biosynthesis pathway. Russ J Plant Physl 55:390–399

Isayenkov S, Mrosk C, Stenzel I, Strack D, Hause B (2005) Suppression of allene oxide cyclase in hairy roots of *Medicago truncatula* reduces jasmonate levels and the degree of mycorrhization with Glomus intraradices. Plant Physiol 139:1401–1410

Jiang K, Liao Z, Pi Y, Huang Z, Hou R, Cao Y, Wang Q, Sun Z, Tang K (2008) Molecular cloning and expression profile of a jasmonate biosynthetic pathway gene allene oxide cyclase from *Hyoscyamus niger*. Mol Biol (Mosk) 42:434–444

Jiang K, Pi Y, Hou R, Jiang L, Sun X, Tang K (2009) Promotion of nicotine biosynthesis in transgenic tobacco by overexpressing allene oxide cyclase from *Hyoscyamus niger*. Planta 229:1057–1063

Ketchum REB, Gibson DM, Croteau RB, Shuler ML (1999) The kinetics of taxoid accumulation in cell suspension cultures of Taxus following elicitation with methyl jasmonate. Biotechnol Bioeng 62:97–105

Knight H (1999) Calcium signaling during abiotic stress in plants. Int Rev Cytol 195:269–324

Kumar S, Tamura K, Jakobsen IB, Nei M (2001) MEGA2: molecular evolutionary genetics analysis software. Bioinformatics 17: 1244–1245

Laudert D, Schaller F, Weiler EW (2000) Transgenic *Nicotiana tabacum* and *Arabidopsis thaliana* plants overexpressing allene oxide synthase. Planta 211:163–165

Liao P, Zhou W, Zhang L, Wang J, Yan X, Zhang Y, Zhang R, Li L, Zhou G, Kai G (2009) Molecular cloning, characterization and expression analysis of a new gene encoding 3-hydroxy-3-methylglutaryl coenzyme A reductase from *Salvia miltiorrhiza*. Acta Physiol Plant 31:565–572

Liu B, Wang W, Gao J, Chen F, Wang S, Xu Y, Tang L, Jia Y (2010) Molecular cloning and characterization of a jasmonate biosynthetic pathway gene for allene oxide cyclase from *Jatropha curcas*. Acta Physiol Plant 32:531–539

Livak KJ, Schmittgen TD (2001) Analysis of relative gene expression data using real-time quantitative PCR and the 2(-Delta Delta C(T)) method. Methods 25:402–408

Maucher H, Hause B, Feussner I, Ziegler J, Wasternack C (2000) Allene oxide synthases of barley (*Hordeum vulgare* cv. Salome): tissue specific regulation in seedling development. Plant J 21:199–213

Murray MG, Thompson WF (1980) Rapid isolation of high molecular weight plant DNA. Nucleic Acids Res 8:4321–4326

Pauwels L, Morreel K, De Witte E, Lammertyn F, Van Montagu M, Boerjan W, Inze D, Goossens A (2008) Mapping methyl jasmonate-mediated transcriptional reprogramming of metabolism and cell cycle progression in cultured Arabidopsis cells. Proc Natl Acad Sci USA 105:1380–1385

Pauwels L, Inzé D, Goossens A (2009) Jasmonate-inducible gene: what does it mean? Trends Plant Sci 14:87–91

Pi Y, Jiang K, Cao Y, Wang Q, Huang Z, Li L, Hu L, Li W, Sun X, Tang K (2009) Allene oxide cyclase from *Camptotheca acuminata* improves tolerance against low temperature and salt stress in tobacco and bacteria. Mol Biotechnol 41:115–122

Robert-Seilaniantz A, Grant M, Jones JDG (2011) Hormone crosstalk in plant disease and defense: more than just jasmonate-salicylate antagonism. Annu Rev Phytopathol 49:317–343

Saitou N, Nei M (1987) The neighbor-joining method: a new method for reconstructing phylogenetic trees. Mol Biol Evol 4:406–425

Sanders D, Brownlee C, Harper JF (1999) Communicating with calcium. Plant Cell Online 11:691–706

Sasaki Y, Asamizu E, Shibata D, Nakamura Y, Kaneko T, Awai K, Amagai M, Kuwata C, Tsugane T, Masuda T (2001) Monitoring of methyl jasmonate-responsive genes in Arabidopsis by cDNA macroarray: self-activation of jasmonic acid biosynthesis and crosstalk with other phytohormone signaling pathways. DNA Res 8:153–161

Schaller F (2001) Enzymes of the biosynthesis of octadecanoid-derived signalling molecules. J Exp Bot 52:11–23

Schaller F, Schaller A, Stintzi A (2004) Biosynthesis and metabolism of jasmonates. J Plant Growth Regul 23:179–199

Seo HS, Song JT, Cheong JJ, Lee YH, Lee YW, Hwang I, Lee JS, Choi YD (2001) Jasmonic acid carboxyl methyltransferase: a key enzyme for jasmonate-regulated plant responses. Proc Natl Acad Sci USA 98:4788–4793

Stenzel I, Hause B, Miersch O, Kurz T, Maucher H, Weichert H, Ziegler J, Feussner I, Wasternack C (2003a) Jasmonate biosynthesis and the allene oxide cyclase family of Arabidopsis thaliana. Plant Mol Biol 51:895–911

Stenzel I, Hause B, Maucher H, Pitzschke A, Miersch O, Ziegler J, Ryan CA, Wasternack C (2003b) Allene oxide cyclase dependence of the wound response and vascular bundle-specific generation of jasmonates in tomato—amplification in wound signalling. Plant J 33:577–589

Strassner J, Schaller F, Frick UB, Howe GA, Weiler EW, Amrhein N, Macheroux P, Schaller A (2002) Characterization and cDNA-microarray expression analysis of 12-oxophytodienoate reductases reveals differential roles for octadecanoid biosynthesis in the local versus the systemic wound response. Plant J 32:585–601

Suzuki H, Reddy MS, Naoumkina M, Aziz N, May GD, Huhman DV, Sumner LW, Blount JW, Mendes P, Dixon RA (2005) Methyl jasmonate and yeast elicitor induce differential transcriptional and metabolic re-programming in cell suspension cultures of the model legume *Medicago truncatula*. Planta 220:696–707

Thompson JD, Gibson TJ, Plewniak F, Jeanmougin F, Higgins DG (1997) The CLUSTAL_X windows interface: flexible strategies for multiple sequence alignment aided by quality analysis tools. Nucleic Acids Res 25:4876–4882

Vick BA, Zimmerman DC (1984) Biosynthesis of jasmonic acid by several plant species. Plant Physiol 75:458–461

Wang C, Avdiushko S, Hildebrand DF (1999) Overexpression of a cytoplasm-localized allene oxide synthase promotes the wound-induced accumulation of jasmonic acid in transgenic tobacco. Plant Mol Biol 40:783–793

Wang X, Cui G, Huang L, Qiu D (2007a) Effects of methyl jasmonat on accumulation and release of tanshinones in suspension cultures of *Salvia miltiorrhiza* hairy root. China J Chin Mater Med 32:300–302 (in Chinese)

Wang X, Morris-Natschke SL, Lee KH (2007b) New developments in the chemistry and biology of the bioactive constituents of Tanshen. Med Res Rev 27:133–148

Wang X, Cui G, Huang L, Gao W, Yuan Y (2009) A full length cDNA of 4-(cytidine 5′-diphospho)-2-C-methyl-derythritol kinase cloning and analysis of introduced gene expression in *Salvia miltiorrhiza*. Acta Pharm Sin 43:1251–1257 (in Chinese)

Wasternack C (2007) Jasmonates: an update on biosynthesis, signal transduction and action in plant stress response, growth and development. Ann Bot 100:681–697

Xiao Y, Gao S, Di P, Chen J, Chen W, Zhang L (2009) Methyl jasmonate dramatically enhances the accumulation of phenolic acids in *Salvia miltiorrhiza* hairy root cultures. Physiol Plant 137:1–9

Yamada A, Saitoh T, Mimura T, Ozeki Y (2002) Expression of mangrove allene oxide cyclase enhances salt tolerance in *Escherichia coli,* yeast, and tobacco cells. Plant Cell Physiol 43:903–910

Yan X, Zhang L, Wang J, Liao P, Zhang Y, Zhang R, Kai G (2009) Molecular characterization and expression of 1-deoxy-D-xylulose 5-phosphate reductoisomerase (DXR) gene from *Salvia miltiorrhiza*. Acta Physiol Plant 31:1015–1022

Yan Y, Wang Z, Tian W, Dong Z, Spencer DF (2010) Generation and analysis of expressed sequence tags from the medicinal plant *Salvia miltiorrhiza*. Sci China Life Sci 53:273–285

Zhao J, Davis LC, Verpoorte R (2005) Elicitor signal transduction leading to production of plant secondary metabolites. Biotechnol Adv 23:283–333

Zhou L, Zuo Z, Chow MS (2005) Danshen: an overview of its chemistry, pharmacology, pharmacokinetics, and clinical use. J Clin Pharmacol 45:1345–1359

Zhu Z, Zhang H, Zhao L, Dong X, Li X, Chai Y, Zhang G (2007) Rapid separation and identification of phenolic and diterpenoid constituents from Radix *Salvia miltiorrhizae* by high-performance liquid chromatography diode-array detection, electrospray ionization time-of-flight mass spectrometry and electrospray ionization quadrupole ion trap mass spectrometry. Rapid Commun Mass Spectrom 21:1855–1865

Ziegler J, Hamberg M, Miersch O, Parthier B (1997) Purification and characterization of allene oxide cyclase from dry corn seeds. Plant Physiol 114:565–573

Ziegler J, Stenzel I, Hause B, Maucher H, Hamberg M, Grimm R, Ganal M, Wasternack C (2000) Molecular cloning of allene oxide cyclase. The enzyme establishing the stereochemistry of octadecanoids and jasmonates. J Biol Chem 275:19132–19138

Ziegler J, Keinänen M, Baldwin IT (2001) Herbivore-induced allene oxide synthase transcripts and jasmonic acid in *Nicotiana attenuata*. Phytochemistry 58:729–738